Available online at www.sciencedirect.com
ScienceDirect
International Journal of Mass Spectrometry 265 (2007) 281–294
International Journal of Mass Spectrometry
www.elsevier.com/locate/ijms

Electrospray ionization of uranyl-citrate complexes: Adduct formation and ion-molecule reactions in 3D ion trap and ion cyclotron resonance trapping instruments

Árpád Somogyi *, Sofie P. Pasilis [1], Jeanne E. Pemberton **

Department of Chemistry, University of Arizona, 1306 East University Boulevard, Tucson, AZ 85721, USA

Received 29 November 2006; received in revised form 26 February 2007; accepted 26 February 2007
Available online 3 March 2007

Abstract

Results presented here demonstrate the usefulness of electrospray ionization and gas-phase ion-molecule reactions to predict structural and electronic differences in complex inorganic ions. Electrospray ionization of uranyl citrate solutions generates positively and negatively charged ions that participate in further ion-molecule reactions in 3D ion trap and FT-ICR mass analyzers. Most ions observed are derived from the major solution uranyl-citrate complexes and involve species of $\{(UO_2)_2Cit_2\}^{2-}$, $(UO_2)_3Cit_2$, and $\{(UO_2)_3Cit_3\}^{3-}$, where Cit indicates the citrate trianion, $C_6H_5O_7{}^{3-}$. In a 3D ion trap operated at relatively high pressure, complex adducts containing solvent molecules, alkali and ammonium cations, and nitrate or chloride anions are dominant, and proton/alkali cation (Na^+, K^+) exchange is observed for up to six exchangeable protons in an excess of alkali cations. Adduct formation in a FT-ICR cell that is operated at lower pressures is less dominant, and direct detection of positive and negative ions of the major solution complexes is possible. Multiply charged ions are also detected, suggesting the presence of uranium in different oxidation states. Changes in uranium oxidation state are detected by He-CID and SORI-CID fragmentation, and certain fragments undergo association reactions in trapping analyzers, forming "exotic" species such as $[(UO_2)_4O_3]^-$, $[(UO_2)_4O_4]^-$, and $[(UO_2)_4O_5]^-$. Ion-molecule reactions with D_2O in the FT-ICR cell indicate substantial differences in H/D exchange rate and D_2O accommodation for different ion structures and charge states. Most notably, the positively charged ions $[H_2(UO_2)_2Cit_2(H)]^+$ and $[(UO_2)_2(Cit)]^+$ accommodate two and three D_2O molecules, respectively, which reflects well the structural differences, i.e., tighter uranyl-citrate coordination in the former ion than in the latter. The corresponding negatively charged ions accommodate zero or two D_2O molecules, which can be rationalized using suggested solution phase structures and charge state distributions. Published by Elsevier B.V.

Keywords: Ion-molecule reaction; Uranyl-citrate complex; Electrospray ionization; Ion trap; FT-ICR; Ion fragmentation

1. Introduction

Recent years have seen a pronounced increase in interest in the gas-phase chemistry of actinide (An) ions. One motivation for these investigations has been to understand the role of 5f electrons in An^{n+} and $AnO_n{}^+$ chemistry [1]. Many of these studies were (and are) limited to uranium and thorium because of the difficulty in handling the more highly radioactive actinides in conventional laboratories, although some research into the gas-phase chemistry of other actinide ions has been completed [1]. Most gas-phase studies involving uranium have focused on reactions of U^+ and UO^+ with alkanes [2,3] and alkenes [4] alcohols, thiols and ethers [5] and arenes [6]. Other studies have demonstrated that U^+ may be easily oxidized by small molecules such as O_2, CO, CO_2, COS, H_2O and D_2O [7–9]. The gas-phase chemistry of uranium in the IV, V, and VI oxidation states, however, is of increasing interest and has been the focus of several recent studies [10–19].

Electrospray ionization (ESI) can be used to generate ions in the U(V) and U(VI) oxidation states from solutions containing these species, and can, in principle, be used to directly interrogate uranium-containing solutions under various chemical conditions. Such studies will hopefully lead to an improved understanding of uranium solution speciation, as well as further important and interesting new research

* Corresponding author. Tel.: +1 520 626 7272; fax: +1 520 626 7272.
** Corresponding author.
E-mail addresses: asomogyi@u.arizona.edu (Á. Somogyi), pembertn@u.arizona.edu (J.E. Pemberton).
[1] Present address: Chemical Sciences Division, Oak Ridge National Laboratory, Oak Ridge, TN 37831-6131, USA.

1387-3806/$ – see front matter. Published by Elsevier B.V.
doi:10.1016/j.ijms.2007.02.050

into the gas-phase chemistry of U(V) and U(VI)-containing species.

The use of ESI-MS to examine U(VI) speciation, U(VI)-ligand stoichiometry and gas-phase chemistry is still relatively new, and therefore, much work remains to elucidate the types of chemical transformations uranium-containing species may undergo during the electrospray process and in the mass spectrometer. Of importance are changes in oxidation state, changes in number or type of coordinating ligand, adduct formation with alkali ions, anions, or solvent molecules, and effects of solvent on the gas phase chemistry of the species of interest. As an additional complicating factor, some of these reactions may be instrument specific, dependent on conditions in trapping instruments or reactions occurring during electrospray ionization or desolvation. Therefore, careful experiments must be carried out using different instrumental techniques to gain a complete understanding of the gas-phase chemistry of U(VI).

Reduction of U(VI) to U(V) has been previously demonstrated during ESI-MS. Agnes and Horlick [20] presented preliminary results for the analytical use of ESI-MS for elemental analysis of metals and detected UO_2^+ as the dominant ion from a solution of uranyl(VI) nitrate, indicating that charge reduction occurred. Moulin et al. [10] compared results from ESI-MS to those obtained using fluorescence spectroscopy to examine the speciation of UO_2^{2+} from a 0.04 mM solution of uranyl perchlorate. They observed the formation of $[(UO_2)(ClO_4)(H_2O)_n]^+$ and $[(UO_2)(OH)(H_2O)_n]^+$ ions (where $n = 0$–3) at pH 2.3 and 3.5, respectively, and ions corresponding to $[(UO_2)(OH)(H_2O)_n]^+$ and $[(UO_2)_3(OH)_5]^+$ at pH 6.8. Interestingly, during collision-induced dissociation (CID) of $[(UO_2)(OH)(H_2O)_n]^+$, the bare ion, UO_2^+, was only observed upon the loss of all coordinating water molecules, suggesting a simple charge transfer from a H_2O ligand with elimination of a H_2O radical. Reduction of U(VI) has also been noted during CID of $[(UO_2)(NO_3)]^+$ and $[(UO_2)(RO)]^+$ (where R = CH_3 or CH_2CH_3) as a result of loss of $NO_3^\bullet$ and $RO^\bullet$ during CID [14].

An additional complication in these studies is that the stoichiometries of U(VI)-ligand complexes may not be conserved during the electrospray process. Lamouroux et al. [12] noted that, while U(VI) is extracted by tributyl phosphate (TBP) in the PUREX process as $UO_2(NO_3)_2(TBP)_2$, exchange of NO_3^- for TBP takes place during ionization, resulting in the appearance of $[(UO_2)(NO_3)(TBP)_3]^+$ in the mass spectrum. Similarly, as discussed previously such as CO_3^{2-} may be extremely labile at the relatively high temperatures required for desolvation, and may be replaced by NO_3^- [21].

U(VI) readily forms complexes or adducts with common anions such as NO_3^- and Cl^-, alkali ions, and gas-phase solvent molecules such as methanol, acetonitrile, acetone and water [13–19,22]. In addition, binding of molecular oxygen to di and triligated UO_2^+ has been shown to occur [19]. Such reactions greatly complicate spectral interpretation.

As a further contribution to studies on aqueous uranyl solution chemistry, the pH dependence of uranyl(VI) complexation by citric acid using Raman and attenuated total reflection FTIR spectroscopies and ESI mass spectrometry was recently reported from this laboratory [23]. In solutions of lower pH (~3–5), a species with the $\{(UO_2)_2(Cit)_2\}^{2-}$ core is formed. In solutions of higher pH (>6.5), this $\{(UO_2)_2(Cit)_2\}^{2-}$ interconverts to form $\{(UO_2)_3(Cit)_3\}^{3-}$ and $(UO_2)_3(Cit)_2$. (Note that for simplicity, Cit is used throughout this paper to indicate the citrate trianion ligand, $C_6H_5O_7^{3-}$. Braces are used to indicate charged solution species, and square brackets are used to indicate gas-phase species detected by the mass analyzers.) ESI-MS studies on solutions of varying uranyl(VI)-citrate ratio, pH and solution counteranion confirm the results on the stochiometry of these complexes. In addition, however, the positive ion spectra also indicate that these uranyl-citrate complexes easily form adducts with H_2O, HNO_3, HCl, NH_4^+, Na^+, and K^+. We have also observed complex positive and negative ion formation for uranyl-nitrate solutions by ESI in an FT-ICR instrument [24].

The complex ion formation observed during the ESI process, as well as the indications of ion-molecule reactions in trapping instruments, inspired us to further extend our studies on uranyl-citrate complexes. In the present study, we focus on ion-molecule reactions involving selected positive and negative uranyl-citrate ions formed by ESI. The results presented here were obtained using two trapping instruments: a three-dimensional ion trap (3D IT) and an FT-ICR instrument. First, we summarize and discuss results obtained in a 3D IT, and follow this with a presentation on H/D exchange and water (D_2O) addition reactions observed in the FT-ICR instrument. Tandem MS/MS experiments on selected adduct ions have also been performed using gas-phase collisional activation with He (in the 3D IT instrument) and sustained off-resonance irradiation (SORI) with N_2 in the FT-ICR instrument. Collectively, these results add to the growing body of knowledge that further documents the rich nature of gas-phase ion-molecule reactions of uranyl-containing species formed during electrospray ionization.

2. Experimental

2.1. Materials

Citric acid (Aldrich, 99.5%; fully protonated form designated as H_3Cit throughout this report), uranyl nitrate (Fluka, 98–102%), and uranyl chloride (All-Chemie Ltd.) were used as received. Water was purified with a Milli-Q UV system (Millipore Corp.). Ammonium hydroxide (Fluka, >99%), Nitric acid (Mallinkrodt, AR, 69.6%) and hydrochloric acid (Baker, ACS Reagent, 36.5–38%) were used for pH adjustment. Acetonitrile (EM Science, 99.99%), methanol (Baker, 99%), and Milli-Q water were used to prepare samples for ESI-MS experiments. Potassium chloride (Aldrich, 99+%), potassium nitrate (Fisher Scientific, >99%), sodium chloride (Mallinkrodt, 99.8%) and sodium nitrate (Mallinkrodt) salts were used to prepare samples for studies involving alkali adducts adduct.

2.2. Solution preparations for ESI-MS experiments

For ion trap studies, solutions of 100 mM citric acid and 100 mM uranyl nitrate were combined in the appropriate ratio, pH-adjusted with NH_4OH, and diluted to a concentration of

~0.5 mM with a 20% (v/v) solution of acetonitrile/water or methanol/water. Uranyl chloride was sometimes used in place of uranyl nitrate in order to examine the effect of counteranion on adduct formation. pH was readjusted as necessary after dilution. For studies of alkali ion interactions with the uranyl citrate complexes, samples were spiked with Na^+ and K^+ for a total alkali ion concentration of 1 mM. For studies of the effect of excess citrate ligand in solution, samples were prepared with a total citrate concentration of 10 mM. For positive ion FTMS studies, solutions were prepared by dilution of aqueous solutions 0.5 mM in uranyl and citrate to a final concentration of 167 μM with methanol, such that the final solvent composition was 67% CH_3OH/33% H_2O (v/v). For negative ion studies, the aqueous solutions were diluted to a concentration of 50 μM with methanol; here the solvent composition was 90% CH_3OH/10% H_2O. The pH of the solutions used for FT-ICR measurements was not measured.

2.3. MS instrumentation

ESI-MS measurements were made using a Thermoelectron (Finnigan) LCQ Classic ion trap mass spectrometer (Thermoelectron Co., San Jose, CA) and a 4.7 T IonSpec Fourier transform ion-cyclotron resonance (FT-ICR) instrument (IonSpec Corp., Lake Forest, CA). Samples were introduced using direct infusion with flow rates of 13 μL/min (ion trap) and 2 μL/min (FT-ICR). All experiments in the ion trap were performed in the positive ion mode, while both positive and negative ion modes were used in the FT-ICR instrument. Typical ESI conditions in the ion trap instruments were as follows: spray voltage: 4.7 kV, capillary voltage: 40 V, capillary temperature: 200 °C, sheath gas: N_2 with a flow rate of 60 (arbitrary units).

The IonSpec 4.7 T FT-ICR was used for high resolution/accurate mass measurements, sustained off-resonance irradiation–collision induced dissociation (SORI-CID) fragmentation of selected positively and negatively charged uranyl-citrate complexes, as well as for ion-molecule reactions of uranyl-citrate ions with D_2O. Positively and negatively charged ions were generated with an Analytica (Branford, CT) second-generation electrospray source. The capillary temperature was kept at 60 °C. For positively charged ions, a needle voltage of 3.8 kV was applied, while −2.5 kV was used in the negative ion mode. The electrospray source is a linear needle-heated capillary arrangement with the needle angle slightly off-axis to reduce contamination. Droplets enter a heated capillary (60 °C) and the ions formed are accumulated in a hexapole/quadrupole ion guide system. The hexapole offset and quadrupole trapping times can be varied, and as expected, complexes with higher molecular weights can be detected with increased trapping times. Detailed and systematic investigation of trapping parameters was not undertaken as one of the main foci of the present work. Typical hexapole accumulation and quadrupole trapping times were 1000 and 3.5 ms (positive mode) and 500 and 3.7 ms (negative mode), respectively. The FT-ICR instrument was modified in-house for ion-molecule reaction studies by incorporating the pulsed-leak configuration described by Jiao et al. [25]. Typical D_2O pressure was (3–5) × 10^{-9} torr with a base pressure in the ICR analyzer of 7 × 10^{-11} torr. For H/D and D_2O addition experiments, all trapped ions except those of interest are ejected from the ICR cell via a chirp frequency sweep. Isolated ions are allowed to cool for a few seconds before the reagent gas (D_2O) is leaked into the analyzer region. After a well-defined reaction time, D_2O was pumped away during a 30 s pump-down to reach the low-pressure region (ca. 3–4 × 10^{-9} torr) necessary for ion detection.

Protonated peptide and polyethylene glycol (positive ion mode) and linear alkylbenzene sulfonate (LAS) (negative ion mode) standards were used to determine the accurate masses of some characteristic ions. These ion masses were then used in further studies as internal calibrant masses to determine elemental composition of additional ions including SORI-CID fragments. Ions used for calibration are noted in the tables.

3. Results and discussion

3.1. Adduct formation of uranyl-citrate complexes with alkali ions (Na^+, K^+) during ESI and in a 3D ion trap

In ESI-MS studies of metal ion solutions containing ligands, it is important to discriminate between complexation reactions occurring in solution, and those occurring during desolvation or in the gas phase. Formation of adducts between alkali metal ions or common solution anions such as chloride and nitrate and the metal–ligand complexes of interest can further complicate the interpretation of ESI spectra. Therefore, experiments must be performed to determine the effects of adduct formation on the mass spectrum, and to facilitate differentiation of adduct species from species related to the metal ion solution chemistry.

Initial ESI-MS studies of solutions of uranyl-citrate complexes indicated the formation of adducts that differed based on the structure of the complex [23]. For example, HNO_3 and HCl adducts form in the gas-phase with $H_2(UO_2)_2Cit_2$ and $(UO_2)_3Cit_2$, but not with $H_3(UO_2)_3Cit_3$ [23]. Similarly, Na^+ was observed to form adducts with $H_2(UO_2)_2Cit_2$ and $(UO_2)_3Cit_2$, which appear as the most intense peaks in the mass spectra of these species, but not with $H_3(UO_2)_3Cit_3$, although this complex does form an adduct with K^+ that shows up as a low-intensity peak in the mass spectrum [23]. In these previous studies, the alkali cations were present in aqueous solutions as contaminant ions and were hypothesized to form adducts with uranyl complexes during desolvation. In order to further investigate this phenomenon, samples of uranyl-citrate complexes were spiked with Na^+ and K^+ and their adduct formation investigated.

$\{(UO_2)_2Cit_2\}^{2-}$ is the most prominent species in a pH 4.0 solution containing 0.5 mM uranyl and 0.5 mM citrate, and in the gas phase, this species can form adducts with Na^+, H_2O, CH_3CN, and HNO_3 or HCl [23]. Although the relative intensities of these cluster ions vary somewhat in replicate analyses, in general, $[(H_2(UO_2)_2Cit_2)(HNO_3)(H_2O)(Na)]^+$ (*m/z* 1024.4) appears as the most intense ion in the spectrum when NO_3^- is the counterion in solution (Fig. 1a, Table 1). (Note that for consistency, the notation suggested originally by Van Stipdonk [17] and applied in our previous paper [24]

Table 1
ESI-MS ion assignments for $H_2(UO_2)_2Cit_2$ complexes and adducts (3D ion trap)[a]

Ion species	Calculated *m/z*	Observed *m/z*	X = Na^+		X = K^+	
			Calculated *m/z*	Observed *m/z*	Calculated *m/z*	Observed *m/z*
$[(H_2(UO_2)_2Cit_2)(NH_4)]^+$	938.1	938.4				
$[(H_2(UO_2)_2Cit_2)(H_2O)(NH_4)]^+$	956.1	955.8				
$[(H_2(UO_2)_2Cit_2)(H_2O)(X)]^+$			961.1	961.5		
$[(H_2(UO_2)_2Cit_2)(H_2O)_2(X)]^+$			979.1	979.1		
$[(H_2(UO_2)_2Cit_2)(CH_3CN)(H_2O)(X)]^+$			1002.1	1002.2		
$[(H_2(UO_2)_2Cit_2)(HNO_3)(H_2O)(X)]^+$			1024.1	1024.4		
$[(H_2(UO_2)_2Cit_2)(HNO_3)(H_2O)(X)_2(-H)]^+$			1046.1	1046.5		
$[(H_2(UO_2)_2Cit_2)(HNO_3)(H_2O)(X)_3(-2H)]^+$			1068.1	1068.3		
$[(H_2(UO_2)_2Cit_2)(HNO_3)(H_2O)(X)_4(-3H)]^+$			1090.0	1090.6		
$[(H_2(UO_2)_2Cit_2)(HNO_3)(H_2O)(X)_5(-4H)]^+$			1112.0	1112.7		
$[(H_2(UO_2)_2Cit_2)(HNO_3)(H_2O)(X)_6(-5H)]^+$			1134.0	1134.7		
$[(H_2(UO_2)_2Cit_2)(HNO_3)(H_2O)(X)_7(-6H)]^+$			1156.0	1156.8		
$[(H_2(UO_2)_2Cit_2)(HNO_3)(X)_2(-H)]^+$					1060.0	1059.6
$[(H_2(UO_2)_2Cit_2)(HNO_3)(X)_3(-2H)]^+$					1098.0	1097.6
$[(H_2(UO_2)_2Cit_2)(HNO_3)(X)_4(-3H)]^+$					1135.9	1135.5
$[(H_2(UO_2)_2Cit_2)(HNO_3)_2(X)_2(-H)]^+$					1123.0	1122.4
$[(H_2(UO_2)_2Cit_2)(HNO_3)_2(X)_3(-2H)]^+$					1161.0	1160.4
$[(H_2(UO_2)_2Cit_2)(HNO_3)_2(X)_4(-3H)]^+$					1198.9	1198.5
$[(H_2(UO_2)_2Cit_2)(HNO_3)_2(X)_5(-4H)]^+$					1236.9	1236.7
$[(H_2(UO_2)_2Cit_2)(HNO_3)_3(H_2O)(H)]^+$			1128.1	1128.5		
$[(H_2(UO_2)_2Cit_2)(HNO_3)_3(H_2O)(X)]^+$			1150.1	1150.6		
$[(H_2(UO_2)_2Cit_2)(HNO_3)_3(H_2O)(X)_2(-H)]^+$			1172.1	1172.7		
$[(H_2(UO_2)_2Cit_2)(H_3Cit)(H)]_2^{2+}$	1113.1	1112.6				
$[(H_2(UO_2)_2Cit_2)(H_3Cit)(NH_4)]^+$	1130.2	1130.1				
$[(H_2(UO_2)_2Cit_2)(HNO_3)_2(NH_4NO_3)(NH_4)]^+$	1144.2	1144.2				
$[(H_2(UO_2)_2Cit_2)(H_2O)(H_3Cit)(X)]^+$			1153.1	1153.2		
$[(H_2(UO_2)_2Cit_2)(H_2O)(H_3Cit)(X^+)_3(-2H)]^+$			1197.1	1197.3		
$[(H_2(UO_2)_2Cit_2)(H_2O)(H_3Cit)(X^+)_4(-3H)]^+$			1219.1	1219.2		
$[(H_2(UO_2)_2Cit_2)(H_2O)(H_3Cit)(X^+)_5(-4H)]^+$			1241.0	1241.3		
$[(H_2(UO_2)_2Cit_2)(H_2O)(H_3Cit)(X^+)_6(-5H)]^+$			1263.0	1263.5		
$[(H_2(UO_2)_2Cit_2)(H_2O)(H_3Cit)(X^+)_7(-6H)]^+$			1285.0	1285.5		
$[(H_2(UO_2)_2Cit_2)(H_3Cit)_2(H)]^+$	1305.2	1304.5				
$[(H_2(UO_2)_2Cit_2)(H_3Cit)_2(X)]^+$			1327.1	1326.4	1343.1	1342.4

[a] Cit denotes $C_6H_5O_7^{3-}$.

is used. Charges on individual moieties in the complexes are not shown in this notation and only the total charge is shown outside the square brackets.) When 1 mM Na^+ is added to a solution containing $\{(UO_2)_2Cit_2\}^{2-}$, a series of Na^+/H^+ exchange reactions occurs such that the acidic protons on $[(H_2(UO_2)_2Cit_2)(HNO_3)(H_2O)(Na)]^+$ are sequentially replaced by Na^+. Ions corresponding to these exchange reactions appear at *m/z* 1046.5, 1068.3, 1090.6, 1112.7, 1134.7 and 1156.8 (Fig. 1b, Table 1). It appears that six of the seven exchangeable protons in this ion can be replaced by Na^+. Although it is impossible to know definitively without exact gas-phase acidity data which protons exchange, two possibilities seem likely. One ion consistent with six exchanges would have one proton come from HNO_3, two from the carboxylic acid groups, two from citrate hydroxyl groups, and one from H_2O. Alternately, one proton could come from HNO_3, two from the carboxylic acid groups, two from H_2O, and one from a citrate hydroxyl group. Replacement of four protons is preferred given that $[(Na_2(UO_2)_2Cit_2)(NaNO_3)(NaOH)(Na)]^+$ at *m/z* 1112.7 is the most prominent ion in the mass spectrum.

Two separate, but minor, series of adduct peaks can also be seen in Fig. 1b. The peaks of the first minor series are marked with a closed triangle. The series starts with an ion at *m/z* 1128.5, assigned to $[(H_2(UO_2)_2Cit_2)(HNO_3)_3(H_2O)(H)]^+$, and continues with $[(H_2(UO_2)_2Cit_2)(HNO_3)_3(H_2O)(Na)]^+$ at *m/z* 1150.6 and $[(H_2(UO_2)_2Cit_2)(HNO_3)_3(H_2O)(Na)_2(-H)]^+$ at *m/z* 1172.7. Peaks of the second minor series are marked with an open diamond. This series corresponds to Na^+/H^+ exchange reactions with $[(H_2(UO_2)_2Cit_2)(H_2O)(H_3Cit)(Na)]^+$ (*m/z* 1153.3) and begins here with $[(H_2(UO_2)_2Cit_2)(H_2O)(H_3Cit)(Na)_3(-2H)]^+$ at *m/z* 1197.3. Replacement of four of the remaining exchangeable protons on this ion with Na^+ results in additional ions at *m/z* 1219.2, 1241.3, 1263.5 and 1285.5. Here, replacement of four and five of the nine total exchangeable protons on $[(H_2(UO_2)_2Cit_2)(H_2O)(H_3Cit)(Na)]^+$ are preferred, as the ions at *m/z* 1241.3 and 1263.5, corresponding to $[(H_2(UO_2)_2Cit_2)(H_2O)(H_3Cit)(Na)_5(-4H)]^+$ and $[(H_2(UO_2)_2Cit_2)(H_2O)(H_3Cit)(Na)_6(-5H)]^+$, respectively, are the most prominent in this series. Again, the hydroxyl protons are proposed as the most likely retained in these species.

As with Na^+, a series of K^+/H^+ exchange reactions also occur when a pH 4.0 solution containing 0.5 mM uranyl and 0.5 mM citrate is made 1 mM in K^+. In this case,

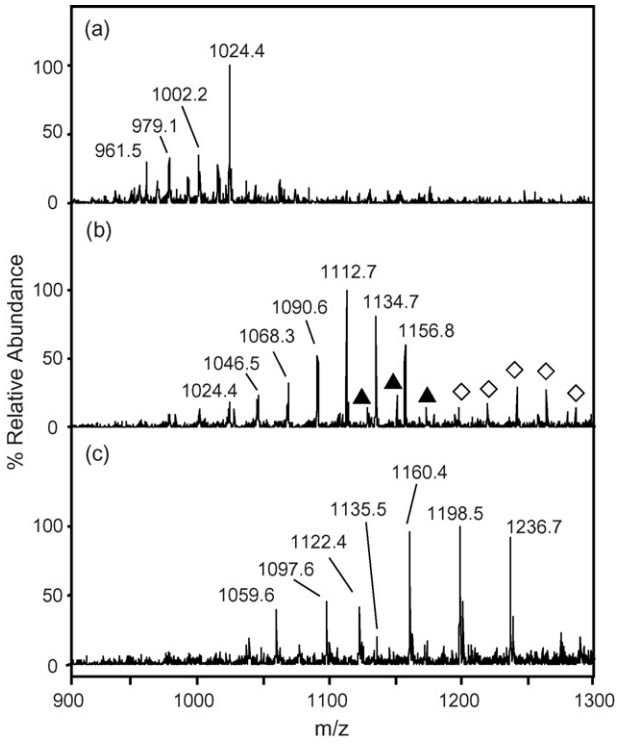

Fig. 1. Positive ion mass spectra (ion trap) showing the formation of alkali ion adducts with $H_2(UO_2)_2Cit_2$. All samples in 20% CH_3CN/80% H_2O at ${}^{s}_{w}$pH 4.0. (a) 0.5 mM UO_2^{2+}, 0.5 mM citrate, 1.0 mM NO_3^-, (b) 0.5 mM UO_2^{2+}, 0.5 mM citrate, 2.0 mM NO_3^-, 1.0 mM Na^+; (▲) and (◊) indicate minor series and (c) 0.5 mM UO_2^{2+}, 0.5 mM citrate, 2.0 mM NO_3^-, 1.0 mM K^+.

two separate series of adducts with ions containing the $H_2(UO_2)_2Cit_2$ species are observed (Fig. 1c). The first series contains peaks at *m/z* 1059.6, 1097.6, and 1135.5, corresponding to the ions $[(H_2(UO_2)_2Cit_2)(HNO_3)(K)_2(-H)]^+$, $[(H_2(UO_2)_2Cit_2)(HNO_3)(K)_3(-2H)]^+$, and $[(H_2(UO_2)_2Cit_2)(HNO_3)(K)_4(-3H)]^+$, respectively. The second, more prominent, series, with peaks at *m/z* 1122.4, 1160.4, 1198.5, and 1236.7 results from the addition of KNO_3 to $[(H_2(UO_2)_2Cit_2)(HNO_3)(K)_2(-H)]^+$, $[(H_2(UO_2)_2Cit_2)(HNO_3)(K)_3(-2H)]^+$, and $[(H_2(UO_2)_2Cit_2)(HNO_3)(K)_4(-3H)]^+$. It is interesting to note that in the presence of K^+, no H_2O adduct with $H_2(UO_2)_2Cit_2$ is formed, although adduct formation with KNO_3 is possible. This behavior is in contrast to that observed with Na^+ in which almost all Na^+-adduct ions also possess at least one H_2O molecule. This difference is consistent with the higher hydration energy of Na^+ relative to K^+. Efforts to further study the hydration effect with Li^+ as the counterion were attempted. Unfortunately, good quality spectra that allowed unambiguous ion assignments could not be obtained from these systems.

As discussed previously [23], $\{(UO_2)_3Cit_3\}^{3-}$ and $\{(UO_2)_3Cit_2\}$ predominate in solution at higher pH. These species form adducts with Na^+ and K^+ in a manner similar to $\{(UO_2)_2Cit_2\}^{2-}$ shown by the assignments provided in Table 2 (spectra not shown). In a solution of 0.6 mM uranyl and 0.4 mM citrate with Cl^- as the counter anion, the base ions $[(H_3(UO_2)_3Cit_3)(H_2O)(H)]^+$ and $[((UO_2)_3Cit_2)(HCl)(H_2O)_2(Na)]^+$ appear at *m/z* 1398.9 and 1283.1, respectively (Table 2). The addition of 1 mM Na^+ to this solution results in the appearance of ions corresponding to two separate series of adducts involving $H_3(UO_2)_3Cit_3$. The more predominant series starts at *m/z* 1420.7 and corresponds to Na^+/H^+ exchange reactions of the type $[(H_3(UO_2)_3Cit_3)(H_2O)(n\mathrm{Na}-(n-1)\mathrm{H})]^+$, where n corresponds to the number of Na^+ ions added. The original ion contains eight exchangeable protons (including three associated with the citrate hydroxyl groups). Six Na^+/H^+ substitutions occur in this series of exchanges, as shown by peaks at *m/z* 1420.7, 1442.9, 1464.8, 1486.7, 1508.8, and 1530.8. Peaks resulting from the first three substitution reactions are most prominent (spectra not shown).

A second, less abundant series beginning at *m/z* 1458.7 corresponds to exchange reactions of the type $[(H_3(UO_2)_3Cit_3)(H_2O)(K)(n\mathrm{Na}^+ - n\mathrm{H})]^+$ (Table 2). The observation of K^+ adducts in solutions containing significant amounts of Na^+ is interesting and may be the result of greater exposure of oxygen atom lone pair electrons in this large uranyl-citrate complex. Here, only four peaks related to Na^+/H^+ exchange are seen, possibly due to the weak signal intensity. Signal intensities of the $[((UO_2)_3Cit_2)(HCl)(H_2O)_2(Na)]$ ion and its adducts are also extremely weak, but peaks at *m/z* 1305.1 and 1327.0 indicate that at least two H^+/Na^+ exchange reactions occur.

When the solution is made 1 mM in K^+, a series of ions corresponding to K^+/H^+ exchange reactions of the type $[(H_3(UO_2)_3Cit_3)(H_2O)(n\mathrm{K}-(n-1)\mathrm{H})]^+$ appear at *m/z* 1436.9, 1474.7, 1512.7, 1550.5 and 1588.5 (Table 2). As for the Na^+ adduct formation described above, six K^+/H^+ exchanges occur. However, no series of adducts analogous to the $[(H_3(UO_2)_3Cit_3)(H_2O)(K)(n\mathrm{Na}-n\mathrm{H})]^+$ species (i.e., $[(H_3(UO_2)_3Cit_3)(H_2O)(\mathrm{Na}+n\mathrm{K}-n\mathrm{H})]^+$) is observed, suggesting that adducts with K^+ are preferred for this uranyl-citrate complex. This conclusion is consistent with the observation that K^+ adducts are observed even in solutions that are 1 mM in Na^+.

Even though the intensities of $[((UO_2)_3Cit_2)(HCl)(H_2O)_2(Na)]^+$ and its adducts are weak, peaks at *m/z* 1298.4, 1321.0 and 1358.6 indicate that at least three H^+/K^+ exchange reactions occur. The observation of Na^+ adducts of the $(UO_2)_3Cit_2$ complex in solutions containing 1 mM K^+ is interesting and suggests a preference of this complex for Na^+ relative to K^+. Since all Na^+ adducts observed under these conditions also contain H_2O, it is impossible to know whether the Na^+ affinity is for $(UO_2)_3Cit_2$ or for H_2O.

3.2. Adduct formation with excess of citric acid

Both $[H_3(UO_2)_3Cit_3]$ and $[H_2(UO_2)_2Cit_2]$ form additional adducts with citric acid when an excess is present in solution. Fig. 2a shows the resulting mass spectrum of a pH 4.0 solution containing 10 mM citrate and 0.5 mM uranyl (assignments in Table 1). Dominant ions at *m/z* 1153.2 and 1304.5 correspond to $[(H_2(UO_2)_2Cit_2)(H_2O)(H_3Cit)(Na)]^+$ and $[(H_2(UO_2)_2Cit_2)(H_3Cit)_2(H)]^+$, respectively. The singly charged ion at *m/z* 1130.1 is assigned to $[(H_2(UO_2)_2Cit_2)(H_3Cit)(NH_4)]^+$. A doubly charged peak is observed at *m/z* 1112.6, albeit with very low intensity, that is assigned to

Table 2
ESI-MS ion assignments for $(UO_2)_3Cit_2$ and $H_3(UO_2)_3Cit_3$ complexes and adducts (3D ion trap)[a]

Ion species	Calculated *m/z*	Observed *m/z*	X = Na^+		X = K^+	
			Calculated *m/z*	Observed *m/z*	Calculated *m/z*	Observed *m/z*
$[(UO_2)_3(C_6H_5O_7)_2(HCl)(H_2O)_2(X)]^+$			1283.1	1283.1	1299.1	1298.4
$[((UO_2)_3Cit_2)(HCl)(H_2O)_2(X^+)_2(-H)]^+$			1305.1	1305.1	1321.1	1321.1
$[((UO_2)_3Cit_2)(HCl)(H_2O)_2(X^+)_3(-2H)]^+$			1327.1	1327.0	1359.0	1358.6
$[(H_3(UO_2)_3Cit_3)(H)]^+$	1381.2	1380.7				
$[(H_3(UO_2)_3Cit_3)(H_2O)(H)]^+$	1399.2	1398.9				
$[(H_3(UO_2)_3Cit_3)(H_2O)(X)]^+$			1421.2	1420.7	1437.1	1436.9
$[(H_3(UO_2)_3Cit_3)(H_2O)(X)_2(-H)]^+$			1443.1	1442.9	1475.1	1474.7
$[(H_3(UO_2)_3Cit_3)(H_2O)(X)_3(-2H)]^+$			1465.1	1464.8	1513.0	1512.7
$[(H_3(UO_2)_3Cit_3)(H_2O)(X)_4(-3H)]^+$			1487.1	1486.7	1551.0	1550.5
$[(H_3(UO_2)_3Cit_3)(H_2O)(X)_5(-4H)]^+$			1509.1	1508.8	1589.0	1588.5
$[(H_3(UO_2)_3Cit_3)(H_2O)(X)_6(-5H)]^+$			1531.1	1530.8	1626.9	1626.3
$[(H_3(UO_2)_3Cit_3)(H_2O)(K)(X)(-H^+)]^+$			1459.1	1458.7		
$[(H_3(UO_2)_3Cit_3)(H_2O)(K)(X)_2(-2H^+)]^+$			1481.1	1480.7		
$[(H_3(UO_2)_3Cit_3)(H_2O)(K)(X)_3(-3H)]^+$			1503.1	1502.4		
$[(H_3(UO_2)_3Cit_3)(H_2O)(K)(X)_4(-4H)]^+$			1525.1	1524.5		
$[(H_3(UO_2)_3Cit_3)(H)(H_3Cit)]^+$	1573.2	1572.5				
$[(H_3(UO_2)_3Cit_3)(H)(H_3Cit)_2]^+$	1765.2	1764.3				

[a] Cit denotes $C_6H_5O_7^{3-}$.

$[(H_2(UO_2)_2Cit_2)(H_3Cit)(H)]_2^{2+}$. The ion at *m/z* 1144.2 is assigned as $[(H_2(UO_2)_2Cit_2)(HNO_3)_2(NH_4NO_3)(NH_4)]^+$. Na^+ or K^+ substitute for H^+ in $[(H_2(UO_2)_2Cit_2)(H_3Cit)_2(H)]^+$ to form the less abundant $[(H_2(UO_2)_2Cit_2)(H_3Cit)_2(Na)]^+$ and $[(H_2(UO_2)_2Cit_2)(H_3Cit)_2(K)]^+$ species at *m/z* 1326.4 and 1342.4, respectively. Although the mass spectrum was scanned to *m/z* 2000, no higher mass species were detected, indicating that adduct formation is limited to two (additional) citric acid molecules.

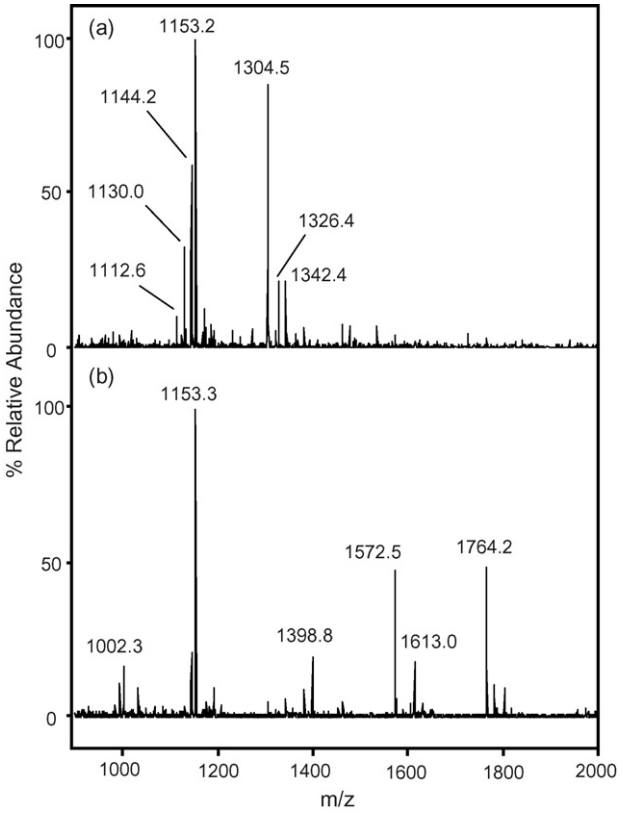

Fig. 2. Positive ion mass spectra (ion trap) showing citric acid adduct formation with $H_2(UO_2)_2Cit_2$ and $H_3(UO_2)_3Cit_3$. All samples in 20% CH_3CN/80% H_2O. (a) 0.5 mM UO_2^{2+}, 10 mM citrate, 1.0 mM NO_3^-, ^s_wpH 4.0, (b) 0.5 mM UO_2^{2+}, 10 mM citrate, 1.0 mM NO_3^-, ^s_wpH 7.7.

Adducts of H_3Cit also appear when an excess of citric acid is present in solutions containing $\{(UO_2)_3Cit_3\}^{3-}$ at pH 7.7 (Fig. 2b, Table 2). Singly charged ions at *m/z* 1572.5 and 1764.3 can be assigned to $[(H_3(UO_2)_3Cit_3)(H_3Cit)(H)]^+$ and $[(H_3(UO_2)_3Cit_3)(H_3Cit)_2(H)]^+$, respectively. A prominent peak at *m/z* 1153.3 for $[(H_2(UO_2)_2(Cit)_2(H_2O)(H_3Cit)(Na)]^+$ is also observed in this spectrum. The observation of a $[H_2(UO_2)_2Cit_2]$ complex at *m/z* 1153 from electrospray of a pH 7.7 solution suggests a decrease in the solution pH during the electrospray process. Such complexes were not observed from electrospray of solutions of similar pH under other solution conditions described above. The solution used for the spectrum shown in Fig. 2b contained excess citric acid; thus, a greater amount of NH_4OH was required for pH adjustment. The decrease in solution pH implied by the observation of $\{(UO_2)_2Cit_2\}^{2-}$ complexes in this spectrum is most likely the result of loss of NH_3 from these solutions during the electrospray process.

It is difficult to unambiguously state from these data whether ions such as $[(H_2(UO_2)_2Cit_2)(H_2O)(H_3Cit)(Na)]^+$ and $[(H_3(UO_2)_3Cit_3)(H_3Cit)_2(H)]^+$ result from a species such as $\{(UO_2)_2Cit_3\}^{5-}$ or $\{(UO_2)_3Cit_5\}^{9-}$ in solution, or if the excess citric acid molecule is simply present as an adduct. However, the measured *m/z* values are ~1 amu less than the theoretical values for the two ions. This may be an indication that these are weakly bound adducts, as it is known that fragile ions exhibit chemical mass shifts of this type [26,27]. Raman spectra of solutions in which there is an excess of citrate do not indicate the existence of any species other than the three already discussed [23]. Since the $\nu_s(UO_2)$ mode is strongly dependent on uranyl coordination, the addition of an excess citrate molecule to the uranyl coordi-

nation sphere would result in a noticeable shift in the $\nu_s(UO_2)$ mode or the presence of additional $\nu_s(UO_2)$ bands. Neither a shift in the $\nu_s(UO_2)$ mode nor new $\nu_s(UO_2)$ bands are observed [23], substantiating the contention that these species are weakly bound adducts with excess citric acid.

3.3. Ion-molecule reactions occurring in a 3D ion trap during CID of uranyl-citrate complexes

CID of metal–ligand complexes can aid in the determination of ion structure. However, in some instances, chemical reactions occurring during CID often involve the loss of small neutral species from large ligands or the loss of intact ligands from metal ions and are not structurally informative [28]. In addition, complex chemical reactions initiated during CID can also complicate structural characterization. In the case of certain metal-containing species, including those containing the uranyl ion, association reactions with adventitious H_2O, NH_3, CH_3OH, and CH_3CN in the ion trap may also occur [14,29,30]. MS and MS/MS data of ions containing the major uranyl-citrate species are discussed here to illustrate some of the complexity involved with the mass spectrometry of uranyl-containing complexes.

3.4. Fragmentation patterns of ions containing $H_2(UO_2)_2Cit_2$ and $H_3(UO_2)_3Cit_3$

Fig. 3a shows the spectrum resulting from a solution 0.5 mM in uranyl and 0.5 mM in citrate at pH 4.0. Although this spectrum and its ions have been shown and discussed previously [23] the spectrum is shown again here for clarity and comparison with related CID spectra. Ion assignments are given in Table 1. As previously discussed, the ion $[(H_2(UO_2)_2Cit_2)(HNO_3)(H_2O)(Na)]^+$ at *m/z* 1024.3 generally predominates when NO_3^- is the counterion in solution.

The fragmentation spectra of the ions at *m/z* 1024.3 and 1002.3 are shown in Fig. 3b and c; assignments are given in Table 1. No adducts of higher *m/z* are formed when either ion is isolated and stored in the ion trap prior to activation, indicating that the parent ions cannot accommodate additional ligands. In our previous work [23] ions appearing at *m/z* 979.0, 961.4, 956.0 and 938.3 were assigned to $[(H_2(UO_2)_2Cit_2)(H_2O)_2(Na)]^+$, $[(H_2(UO_2)_2Cit_2)(H_2O)(Na)]^+$, $[(H_2(UO_2)_2Cit_2)(H_2O)(NH_4)]^+$, and $[(H_2(UO_2)_2Cit_2)(NH_4)]^+$, respectively. The ion at *m/z* 1002.3 can be assigned to $[(H_2(UO_2)_2Cit_2)(H_2O)(CH_3CN)(Na)]^+$.

The presence of ions of the same *m/z* in the fragmentation spectrum as in the parent ion spectrum is unusual and may be the result of what are formally ligand exchange reactions that can occur with other gas-phase molecules present in the ion trap. Thus, collisional activation and dissociation of one species could result not only in fragmentation of the selected ion, but also in the formation of new ions as small molecules present in the trap react with an ion containing the $H_2(UO_2)_2Cit_2$ core. The ion trap has a relatively high operating pressure of $\sim 10^{-5}$ torr, and it is known that common ESI solvents such as H_2O and CH_3OH can make up a significant fraction of the gas in the ion trap. NH_3 is also a likely constituent of the background

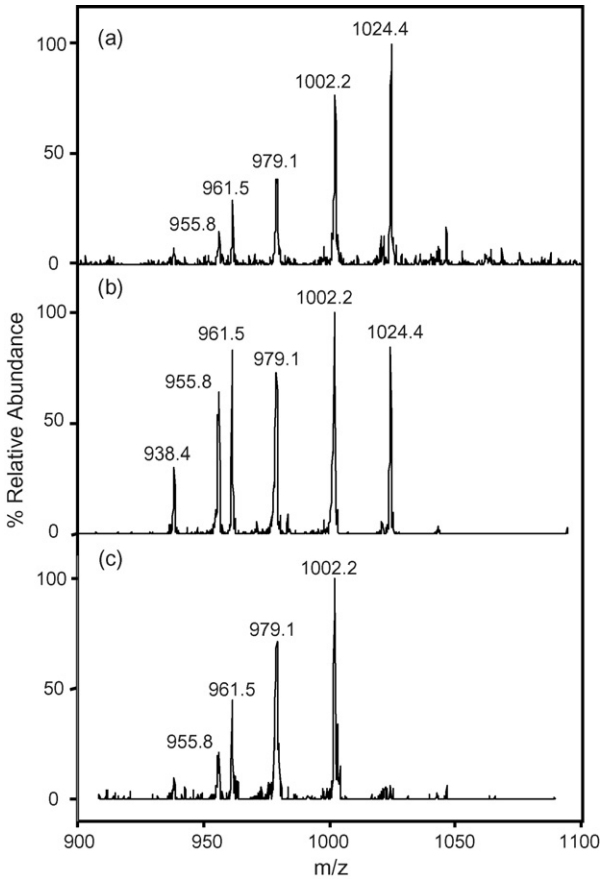

Fig. 3. Positive ion mass spectra (ion trap) of a pH 4.0 solution 0.50 mM in UO_2^{2+} and 0.50 mM in citrate (20% CH_3CN/80% H_2O) showing fragmentation patterns of $H_2(UO_2)_2Cit_2$-containing ions. (a) Full mass spectrum showing adducts of $H_2(UO_2)_2Cit_2$, (b) CID of *m/z* 1024.3 and (c) CID of *m/z* 1002.3.

gas in the ion trap since the starting solutions are pH-adjusted with NH_4OH. Previous work has demonstrated that these neutral molecules react with complexes containing platinum and silver ions [29–31] and uranyl-containing species are also known to readily accept water, methanol, and acetone as ligands via gas-phase association reactions [14–16]. Thus, ions are formed by dissociation, association, and exchange reactions during CID, which adds to the complexity of MS^n spectra.

Upon collisional activation $[(H_2(UO_2)_2Cit_2)(HNO_3)(H_2O)(Na)]^+$ (*m/z* 1024.4) can lose HNO_3 to form $[(H_2(UO_2)_2Cit_2)(H_2O)(Na)]^+$ (*m/z* 961.4), lose HNO_3 and add CH_3CN to form $[(H_2(UO_2)_2Cit_2)(CH_3CN)(H_2O)(Na)]^+$ (*m/z* 1002.3), and lose HNO_3 and gain H_2O to form $[(H_2(UO_2)_2Cit_2)(H_2O)_2(Na)]^+$ (*m/z* 979.0). The presence of ions at *m/z* 938 and *m/z* 956.0 is more difficult to explain (see below).

The fragmentation spectrum resulting from collisional activation of $[(H_2(UO_2)_2Cit_2)(CH_3CN)(H_2O)(Na)]^+$ (*m/z* 1002.3) is equally interesting (Fig. 3c). Loss of CH_3CN, followed by addition of H_2O can explain the presence of $[(H_2(UO_2)_2Cit_2)(H_2O)_2(Na^+)]^+$ (*m/z* 979.0), and loss of CH_3CN leads to $[(H_2(UO_2)_2Cit_2)(H_2O)(Na^+)]^+$ (*m/z* 961.4). However, we again see the formation of an ion at *m/z* 956. Formation of ions at *m/z* 938 and 956 during MS/MS of

m/z 1024 and 1002 can also be explained by an elimination of a neutral Na, as has been described by Vaisar et al. for oxidation of metal-peptide complexes [32,33]. In this case, $[(H_2(UO_2)_2Cit_2)(CH_3CN)(H_2O)(Na)]^+$ (*m/z* 1002.3) would lose Na and CH_3CN to form $[(H_2(UO_2)_2Cit_2)(H_2O)]^+$ (*m/z* 938), followed by the gain of H_2O to form $[(H_2(UO_2)_2Cit_2)(H_2O)_2]^+$ (*m/z* 956). Unfortunately, the low resolution and inadequate mass accuracy of the ion trap analyzer does not allow unambiguous description of these processes.

The CID fragmentation pattern of ions containing the trimeric uranyl-citrate species, $H_3(UO_2)_3Cit_3$ is far less complex than those of ions containing $H_2(UO_2)_2Cit_2$ (spectra not shown). The major ion occurring at *m/z* 1398.8 has been assigned to $[(H_3(UO_2)_3Cit_3)(H_2O)(H)]^+$ [23]. Application of collision energy results in the appearance of ions of *m/z* 1380.8, 1308.7, 1294.7, 1290.7, 1264.8, and 1218.8 (Table 3). The ion of *m/z* 1380.7 is clearly the result of loss of H_2O from the parent ion. The ion of *m/z* 1308.8 occurs at 90 amu less than 1398.8 and is proposed to be the result of decarboxylation reactions involving a loss of CH_2O_2 and CO_2. The ion of *m/z* 1218.8 also appears to be the result of decarboxylation reactions, with losses of two CH_2O_2 and two CO_2 molecules from the $[(H_3(UO_2)_3Cit_3)(H_2O)(H^+)]^+$ parent. The ion of *m/z* 1294.7 may formally correspond to a loss of CH_2COO and CH_2O_2 from the parent. CID of *m/z* 1308.8 results in the loss of H_2O (*m/z* 1290.8), CO_2 (*m/z* 1264.8), CO_2 and CH_2O_2 (*m/z* 1218.7), and possibly CH_2COO and CH_2O_2 (*m/z* 1204.8). It appears that at least four of the nine carboxylate groups can be lost without complete dissociation of the ion, which would be indicated by the presence of ions of lower *m/z* containing the uranyl moiety. This is added evidence for the participation of the citrate hydroxyl groups in bonding to UO_2^{2+}. Presumably, the loss of carboxylate groups means that $[H_3(UO_2)_3Cit_3(H_2O)H]^+$ is undergoing a number of electron transfer and rearrangement reactions during fragmentation, although the charge state of the product ion is maintained. Although the loss of water is also observed from the *m/z* 1399 and 1309 ions, the extensive "decarboxylation" implies that H_2O may be unusually tightly bond in these ions or that hydrolysis of these ions has occurred. Unfortunately, without detailed structural information about the starting $H_3(UO_2)_3Cit_3$ species, the data described here are not sufficient to develop a mechanism for these reactions.

During the isolation step in the ion trap, energy is applied by adjusting the RF voltage amplitudes and by applying multi-frequency resonance ejection waveforms to eject ions of *m/z* values other than that of the selected parent ion. However, some energy can also be imparted to the parent ion during this process, and if the parent ion is fragile, collisions with the buffer gas can cause fragmentation to occur [27]. The excited parent ion may also undergo ligand exchange reactions with small neutral molecules in the ion trap. Solvent molecules such as CH_3OH, CH_3CN, and H_2O may comprise a significant fraction of the buffer gas, and other small neutral molecules, such as NH_3 may be present as well. Here, because NH_4OH was used in these experiments to adjust solution pH, NH_3 could result from deprotonation of solution NH_4^+ during electrospray or during CID of NH_4^+-containing ions [34].

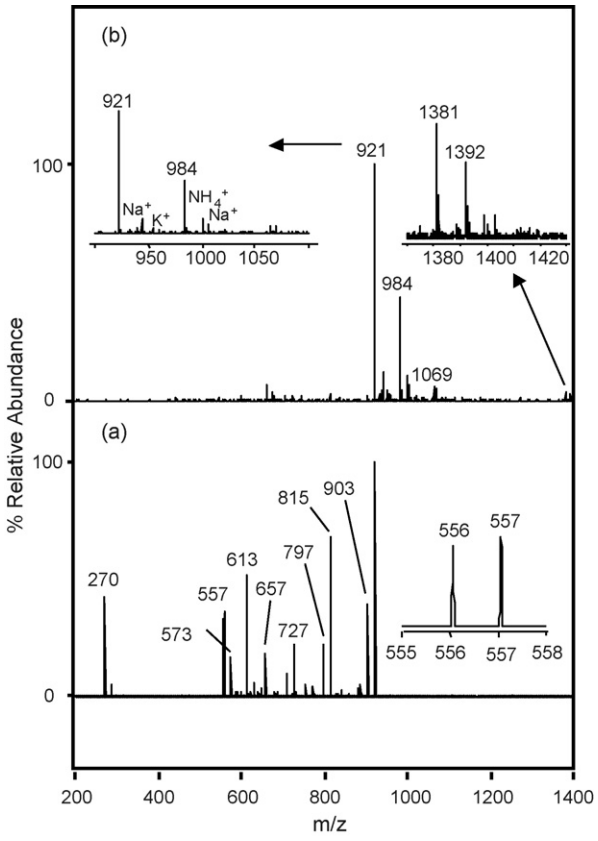

Fig. 4. FT-ICR spectra obtained for a solution 0.167 mM in UO_2^{2+} and 0.167 mM in citrate (67% CH_3OH/ 33% H_2O). (a) Full mass spectrum and (b) 4 V SORI-CID (N_2) spectrum of *m/z* 921, $[H_2(UO_2)_2(Cit)_2(H^+)]^+$. In this case, a NO_3^- counter anion occurred in solution.

The high operating pressure of the ion trap makes the use of the 3D ion trap instrument for the study of these very reactive uranyl species somewhat problematic. On the other hand, these undesirable ion-molecule reactions indicate the chemical complexity of the uranyl-containing ions. The use of an FT-ICR instrument provides an alternate way to study these uranyl complexes at lower pressure and under more controlled conditions. In the following section, we summarize some additional results obtained for uranyl-citrate complexes in an FT-ICR cell. Special attention was given to ion-neutral associations, ion dissociation and exchange reactions with D_2O.

3.5. Positively and negatively charged uranyl-citrate complexes, their fragments and ion-molecule reaction products detected by FT-ICR

Fig. 4a shows a full mass spectrum of a solution containing 0.167 mM uranyl and 0.167 mM citrate. The most intense peaks along with significant fragment ions are collected in Table 4. (Since calculated and measured *m/z* values are also shown in Tables 4 and 5, for better clarity, more detailed elemental compositions are given in the ion species column.) The two most intense ions observed are $[H_2(UO_2)_2(Cit)_2(H)]^+$ (*m/z* 921) and $[H_2(UO_2)_2(Cit)_2(HNO_3)(H)]^+$ (*m/z* 984). Related sodiated, ammoniated, and potassiated ions are also observed.

Table 3
Fragmentation products of m/z 1399, $[H_3(UO_2)_3(C_6H_5O_7)_3(H_2O)H]^+$ (3D ion trap)

Parent ion	Loss associated with fragmentation	Calculated *m/z*	Observed *m/z*
$[H_3(UO_2)_3(C_6H_5O_7)_3(H_2O)H]^+$		1399.2	1398.8
	$-H_2O$	1381.2	1380.8
	$-[HCOOH + CO_2]$	1309.2	1308.7
	$-[CH_2COO + HCOOH]$	1295.2	1294.7
	$-[HCOOH + CO_2 + H_2O]$	1291.2	1290.7
	$-[HCOOH + 2CO_2]$	1265.2	1264.8
	$-[2\ HCOOH + 2CO_2]$	1219.2	1218.8
	$-[CH_2COO + 2HCOOH + CO_2]$	1205.2	1204.8

Using the high resolution FT-ICR instrument, doubly charged ions were unambiguously detected at *m/z* 1381 and 1392; these can be assigned as $[(H_3(UO_3)_2(Cit)_3)_2(H)_2]^{2+}$ and $[(H_3(UO_3)_2(Cit)_3)_2(H)(Na)]^{2+}$, respectively. Thus, dimerization of the uranyl-citrate trimer can occur under these experimental conditions, indicating the existence of relatively stable complexes of high mass. Overall, however, the FT-ICR mass spectra are much simpler than those obtained in the 3D ion trap instrument, indicating the predominance of ion molecule reactions in the latter case.

Fig. 4b shows the SORI-CID (N_2) MS/MS spectrum obtained for the singly charged uranyl-citrate dimer at *m/z* 921, $[H_2(UO_2)_2(Cit)_2(H)]^+$. A detailed list of fragment ions can be found in Table 4. One characteristic feature of this fragmentation spectrum is that no direct loss of one intact citrate ligand is evident. This can be rationalized by the suggested structure for the neutral dimer in solution, $H_2(UO_2)_2(Cit)_2$ [23,35–37] which exhibits strong carboxyl binding to the UO_2 units and relatively free CH_2COOH side chains. The loss of H_2O (*m/z* 903) and double decarboxylation (loss of two CO_2, *m/z* 815) suggests that the gas-phase protonated structure resembles the structure of the neutral. The presence of the singly charged uranyl monomer (*m/z* 270) and peroxo-bonded dimers such as $[(UO_2)_2O]^+$ (*m/z* 556), $[(UO_2)_2OH]^+$ (*m/z* 557) and $[(UO_2)_2O_2H]^+$ (*m/z* 573) indicate changes in uranium oxidation state and strong interactions between uranyl cores even in the absence of citrate ligands. The formation of these ions is difficult to explain, but we assume that they are formed by oxidation reactions between the singly

Table 4
Positively charged uranyl-citrate complex ions and their fragments detected by FT-ICR

Ion species	Loss associated with fragmentation[a]	Calculated *m/z*	Observed *m/z*
MS spectrum			
$[H_2(UO_2)_2(C_6H_5O_7)_2H]^+$		921.1118	921.1118[b]
$[H_2(UO_2)_2(C_6H_5O_7)_2Na]^+$		943.0937	943.1059
$[H_2(UO_2)_2(C_6H_5O_7)_2K]^+$		959.0676	959.0794
$[H_2\ (UO_2)_2(C_6H_5O_7)_2(HNO_3)H]^+$		984.1074	984.1093
$[H(UO_2)_2(C_6H_5O_7)_2(HNO_3)(NH_4)H]^+$		1001.1339	1001.1340
$[H(UO_2)_2(C_6H_5O_7)_2(HNO_3)(Na)H]^+$		1006.0893	1006.0900
$[H(UO_2)_2(C_6H_5O_7)_2(2HNO_3)(NH_4)H]^+$		1064.1296	1064.1377
$[H(UO_2)_2(C_6H_5O_7)_2(2HNO_3)(Na)H]^+$		1069.0850	1069.0954
$[((UO_2)_3(C_6H_5O_7)_3H_3)_2H_2]^{2+}$		1381.1587	1381.1831
$[((UO_2)_3(C_6H_5O_7)_3H_3)_2HNa]^{2+}$		1392.1547	1392.1734
MS/MS of *m/z* 921 $[(UO_2)_2(C_6H_5O_7)_2H_3]^+$[b]			
$[(UO_2)]^+$		270.0406	270.0406[b]
$[(UO_2)OH]^+$		287.0433	287.0434
$[(UO_2)_2O]^+$		556.0761	556.0761
$[(UO_2)_2OH]^+$		557.0840	557.0836
$[(UO_2)_2O_2H]^+$		573.0789	573.0791
$[(UO_2)_2C_3H_5O_2]^+$	–Cit–$2CO_2$–CO	613.1102	613.1109
$[(UO_2)_2C_3H_5O_3]^+$		629.1053	613.1051
$[(UO_2)_2C_4H_5O_4]^+$	–Cit–CO_2–CO	657.1000	657.0992
$[H_2(UO_2)_2(C_8H_6O_4)H]^+$	–$4CO_2$–$2H_2O$	709.1314	709.1329
$[H_2(UO_2)_2(C_8H_8O_5)H]^+$	–$4CO_2$–H_2O	727.1419	727.1434
$[H_2(UO_2)_2(C_9H_6O_6)H]^+$	–$3CO_2$–$2H_2O$	753.1211	753.1204
$[H_2(UO_2)_2(C_9H_8O_7)H]^+$	–$3CO_2$–H_2O	771.1317	771.1340
$[H_2(UO_2)_2(C_{10}H_6O_8)H]^+$	–$2CO_2$–$2H_2O$	797.1110	797.1110
$[H_2(UO_2)_2(C_{10}H_8O_9)H]^+$	–$2CO_2$–H_2O	815.1215	815.1196
$[H_2(UO_2)_2(C_{11}H_6O_{10})H]^+$	–CO_2–$2H_2O$	841.1008	841.1060
$[H_2(UO_2)_2(C_{12}H_6O_{12})H]^+$	–$2H_2O$	885.0908	885.0861
$[H_2(UO_2)_2(C_{12}H_8O_{13})H]^+$	–H_2O	903.1012	903.0994

[a] Cit denotes $C_6H_5O_7^{3-}$.
[b] Ions used for internal calibration.

Table 5
Negatively charged uranyl-citrate complex ions and their fragments detected by FT-ICR

Ion species	Loss associated with fragmentation[a]	Calculated *m/z*	Observed *m/z*
MS spectrum			
$[(UO_2)(OOCCOCH_2CH_2)]^-$		370.0567	370.0573
$[(UO_2)_2(C_6H_5O_7)_2]^{2-}$		459.0441	459.0441[b]
$[(UO_2)_2(C_6H_4O_7)]^-$		728.0769	728.0786
$[(UO_2)_2(C_6H_5O_7)(CH_3OH)]^-$		760.1032	760.1042
$[(UO_2)_2(C_6H_5O_7)_2H]^-$		919.0961	919.0961[b]
$[((UO_2)_2(C_6H_5O_7)_2)_2HNa]^{2-}$		930.0871	930.0985
$[((UO_2)_2(C_6H_5O_7)_2)_2Na_2]^{2-}$		941.0781	941.0901
MS/MS of *m/z* 370 $[(UO_2)(OOCCOCH_2CH_2)]^-$			
$[(UO_2)O]^-$		286.0365	286.0352
$[(UO_2)O_2]^-$		302.0304	302.0301
$[(UO_2)O_2H]^-$		303.0383	303.0381
$[(UO_2)(COCH_2CH_2)]^-$	$-CO_2$	326.0668	326.0665
$[(UO_2)_2O_2]^-$		572.0710	572.0712
$[(UO_2)_2O_3]^-$		588.0660	588.0656
$[(UO_2)_2O_3H]^-$		589.0758	589.0738
MS/MS of *m/z* 459 $[(UO_2)_2(C_6H_5O_7)_2]^{2-}$			
$[(UO_2)O_2]^-$		302.0304	302.0300
$[(UO_2)O_2H]^-$		303.0383	303.0378
$[(UO_2)(CO_2CH_2CH_2)H]^-$		343.0696	343.0691
$[(UO_2)(CO_2COCH_2CH_2)H]^-$		371.0645	371.0639
$[(UO_2)_2(C_{10}H_8O_9)]^{2-}$	$-2CO_2-H_2O$	406.0490	406.0484
$[(UO_2)_2(C_{12}H_8O_{13})]^{2-}$	$-H_2O$	450.0389	450.0383
$[(UO_2)_2O_2]^-$		572.0710	572.0707
$[(UO_2)_2O_3]^-$		588.0660	588.0655
$[(UO_2)_2O_3H]^-$		589.0758	589.0735
$[(UO_2)_4O_3]^-$		1128.1472	1128.1472[b]
$[(UO_2)_4O_4]^-$		1144.1421	1144.1430
$[(UO_2)_4O_5]^-$		1160.1370	1160.1390
MS/MS of *m/z* 728 $[(UO_2)_2(C_6H_4O_7)]^-$[b]			
$[(UO_2)O_2]^-$		302.0304	302.0301
$[(UO_2)O_2H]^-$		303.0383	303.0379
$[(UO_2)_2O]^-$		556.0761	556.0764
$[(UO_2)_2O_2]^-$		572.0710	572.0703
$[(UO_2)_2O_3]^-$		588.0660	588.0655
$[(UO_2)_2O_3H]^-$		589.0758	589.0734
$[(UO_2)_2O_4]^-$		604.0609	604.0605
$[(UO_2)_2(C_4H_4O_3)]^-$	$-2CO_2$	640.0973	640.0971
$[((UO_2)_2(C_5H_3O_5))_2]^{2-}$	dimer–2HCOO	683.0793	683.0975
$[(UO_2)_2(C_5H_4O_5)]^-$	$-CO_2$	684.0871	684.0868
$[(UO_2)_3O_3]^-$		858.1066	858.1059
$[(UO_2)_3O_4]^-$		874.1015	874.1011
$[(UO_2)_3O_5]^-$		890.0964	890.0943
$[(UO_2)_4O_3]^-$		1128.1472	1128.1450
$[(UO_2)_4O_4]^-$		1144.1421	1144.1410
$[(UO_2)_4O_5]^-$		1160.1370	1160.1380
MS/MS of *m/z* 919 $[(UO_2)_2(C_6H_5O_7)_2H]^-$[b,c]			
$C_6H_5O_7^-$		191.0192	191.0192[b]
$[(UO_2)O_2]^-$		302.0304	302.0300
$[(UO_2)O_2H]^-$		303.0383	303.0379
$[(UO_2)_2O_2]^-$		572.0710	572.0706
$[(UO_2)_2O_3]^-$		588.0660	588.0650
$[(UO_2)_2O_3H]^-$		589.0758	589.0731
$[(UO_2)_4(C_6H_5O_7)_2(C_4H_2O_2)]^{2-}$	$-Cit^- - 2H_2O - CO_2 - CO$	770.0875	770.0878
$[(UO_2)_4(C_6H_5O_7)_2(C_6H_2O_5)]^{2-}$	$-Cit^- - 2H_2O$	806.0799	806.0813
$[(UO_2)_2(C_5H_4O_5)_2H]^-$	$-2HCO_2$	829.1008	829.1018
$[(UO_2)_2(C_6H_5O_7)(C_6H_3O_5)H]^-$	$-H_2O$	901.0855	901.0866
$[(UO_2)_4O_3]^-$		1128.1472	1128.1410
$[(UO_2)_4O_4]^-$		1144.1421	1144.1350
$[(UO_2)_4O_5]^-$		1160.1370	1160.1330

[a] Cit denotes $C_6H_5O_7^{3-}$.
[b] Ions used for internal calibration.
[c] The ion at *m/z* 919 is "contaminated" with a small amount of doubly charged dimmer dianion $[(H(UO_2)_2(C_6H_5O_7)_2)_2]^{2-}$.

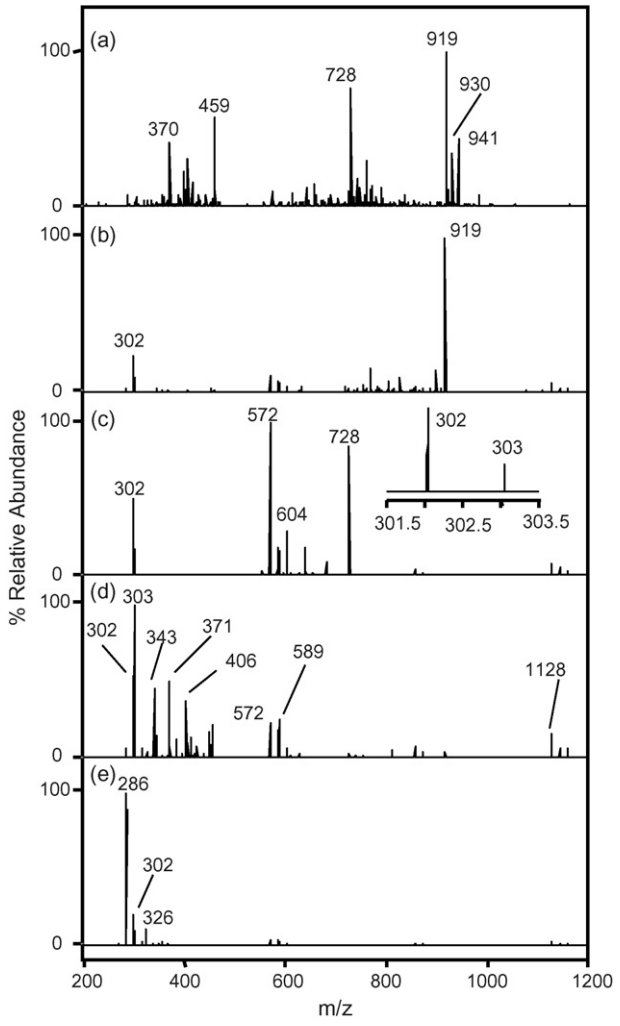

Fig. 5. (a) Negative FT-ICR mass spectrum of a solution of 0.05 mM in UO_2 and 0.05 mM in citrate (90% CH_3OH/10% H_2O). SORI-CID (N_2) fragmentation spectra of (b) the singly charged anion $[H(UO_2)_2(Cit)_2]^-$ (*m/z* 919), (c) the singly charged anion $[H(UO_2)_2(Cit)]^-$ (*m/z* 728), (d) the doubly charged $[H(UO_2)_2(Cit)_2]^{2-}$ anion (*m/z* 459), and (e) the singly charged $[(UO_2)(OOC)C(O)CH_2CH_2]^-$ anion (*m/z* 370).

charged UO_2^+ fragment (*m/z* 270) and oxygen and/or citric acid in the ICR cell. In any case, "peeling off" of both citrate ligands (but leaving the "bridging" oxygen(s) behind) seems to be a general feature of uranyl complex fragmentation by SORI, based on the observation of identical ions from uranyl nitrate complexes as well [24].

A typical negative ion spectrum together with the SORI-CID fragmentation spectra of the most intense anions are shown in Fig. 5. The assignments for the most intense ions along with the SORI-CID fragments (see below) are listed in Table 5. In the negative ion spectrum of Fig. 5, four ions with considerable intensity are observed: $[H(UO_2)_2(Cit)_2]^-$ (*m/z* 919), $[(UO_2)_2(C_6H_4O_7)]^-$ (*m/z* 728), the doubly charged $[(UO_2)_2(Cit)_2]^{2-}$ anion (*m/z* 459), and $[(UO_2)(OOC)C(O)CH_2CH_2]^-$ (*m/z* 370). (Here, again, Cit denotes $C_6H_5O_7$.) The negatively charged monocitrate species, $[(UO_2)_2(C_6H_4O_7)]^-$ appears to exist either as a radical anion or with one uranium atom in the (V) oxidation state. Adducts with Na^+ (*m/z* 941) or methanol (*m/z* 760) are also observed, together with several lower intensity ions. A sodium adduct to the uranyl-citrate non-covalent dimer is detected as a doubly charged ion at *m/z* 930 $[((UO_2)_2(Cit)_2)_2(H)(Na)]^{2-}$. The presence of all of these species indicates complex ion formation processes in the negative ion mode. As representative examples, we focus here only on fragmentation of the four main anions mentioned above.

The SORI-CID spectrum of the uranyl citrate dimer anion, $[H(UO_2)_2(Cit)_2]^-$ (*m/z* 919) shows ions associated with the loss of water (*m/z* 901), double decarboxylation (*m/z* 829), and the formation of oxygen bonded uranyl $[(UO_2)_2O_2]^-$ (*m/z* 572) and "oxygenated" uranyl anions, e.g. $[(UO_2)O_2]^-$ (*m/z* 302). (For a more detailed list of fragment ions, see Table 5.) It is interesting to note that a related ion of $[(UO_2)_2O_2H]^+$ (*m/z* 573) also appears as a positively charged ion (see above and Table 4) suggesting a change in uranyl oxidation state. Although not evident in the spectra in Fig. 5b–e, anions with higher *m/z* values are also present in the SORI-CID fragmentation spectra. The most prominent ion series appears at *m/z* 1128, 1144, and 1160 and can be assigned as $[(UO_2)_4O_3]^-$, $[(UO_2)_4O_4]^-$, and $[(UO_2)_4O_5]^-$, respectively. For completeness, we note that the singly charged ions at *m/z* 919 are "contaminated" with a small amount of doubly charged ions of $[(H(UO_2)_2(Cit)_2)_2]^{2-}$ as indicated by the first isotope peak at ~0.5 *m/z* units higher than the base peak. Therefore, formation of multi-U species can be rationalized by fragmentation of this dimer–dimer dianion. However, multi-uranyl fragments are also detected for the selected ions at *m/z* 728 (Fig. 5c) and 370 (Fig. 5e) that are exclusively singly charged anions with no trace of doubly charged ions. We assume, therefore, that the appearance of these and related multi-uranyl oxygenated anions is indicative of sufficient time for association of these complexes under the experimental conditions used for these studies. These "highly oxygenated" ions also clearly indicate the appearance of uranyl with the uranium in different oxidation states, consistent with the previous observation by Groenewold et al. [19] that molecular oxygen can bind to UO_2^+. Binding of molecular oxygen may be occurring in these uranyl-citrate systems as well, since molecular (or atomic) oxygen is assumed present in the ICR cell due to fragmentation of the citrate ligand. It is not possible to unambiguously derive the oxidation state of U in these complexes. However, if it is assumed that all O species are generally found as O^{2-}, then $[(UO_2)_4O_3]^-$ would possess three U(V) and one U(VI), $[(UO_2)_4O_4]^-$ would contain three U(VI) and one U(V), and $[(UO_2)_4O_5]^-$ would have four U(VI) with one O^{1-}. Alternately, if it is assumed that one molecular O_2 is present, then $[(UO_2)_4OO_2]^-$ would be comprised of three U(IV) and one U(V), $[(UO_2)_4OOO_2]^-$ would possess one U(IV) and three U(V), and $[(UO_2)_4OOOO_2]^-$ would have three U(V) and one U(VI). The combination of possible oxidation states that would occur with bound O being doubly negatively charged is more reasonable that those that would occur if one molecular O_2 species were present. Thus, we conclude that bound O^{2-} is the more likely scenario.

Overall, we conclude that the general features of the anion fragmentation behavior are similar (see list in Table 5), indicat-

ing the preferred formation of predominantly oxygenated uranyl anions without the citrate ligand in MS^2 fragmentation reactions of this type.

3.6. Ion molecule reactions in the FT-ICR cell between positively and negatively charged uranyl-citrate complexes and D_2O

To obtain further information about the stability and saturation of uranyl-citrate complexes, ion-molecule reactions with D_2O were also performed in the FT-ICR cell. These reactions have been demonstrated to be useful in probing interactions between multidentate ligands and metals in gas-phase metal complexes, for example, by Vachet et al. [38–42]. Fig. 6a–c shows the spectra obtained for different reaction times between D_2O and the positively charged $[H_2(UO_2)_2(Cit)_2(H)]^+$ (*m/z* 921). For sake of comparison, the spectrum obtained after a 180 s reaction time between D_2O and the corresponding anion, $[H(UO_2)_2(Cit)_2]^-$ (*m/z* 919) is also shown (Fig. 6d). The spectral changes in Fig. 6a–c clearly show that with increasing reaction time more H/D exchange and D_2O additions occur. Under our experimental conditions, two D_2O molecules are "attached" to the positively charged uranyl-citrate dimer complex (see inset in Fig. 6c). The accumulation of two D_2O molecules can easily be rationalized based on the known structure for the neutral $[H_2(UO_2)_2(Cit)_2]$ complex [23,35–37]. At the 180 s reaction

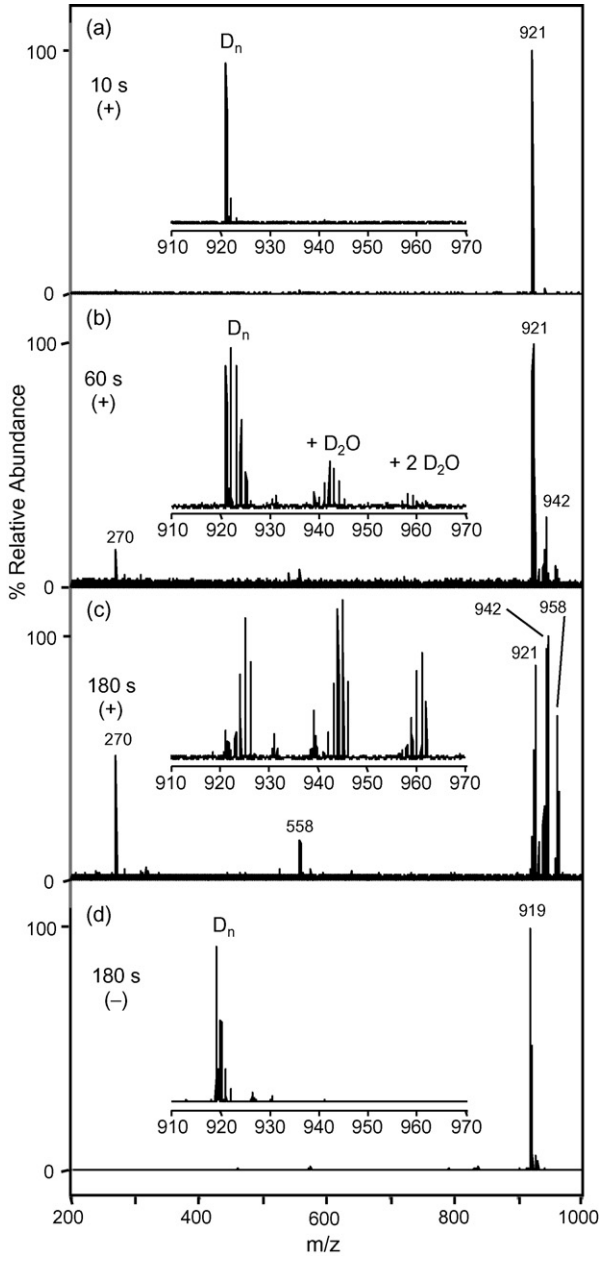

Fig. 6. FT-ICR mass spectrum showing ion-molecule reactions between D_2O and monoisotopically selected uranyl-citrate dimer 1:1 complexes. Reaction times applied for the cation, $[H_2(UO_2)_2(Cit)_2(H)]^+$ (*m/z* 921) (a) 10s, (b) 60s, (c) 180 s, and (d) 180s for the corresponding anion, $[H(UO_2)_2(Cit)_2]^-$ (*m/z* 919).

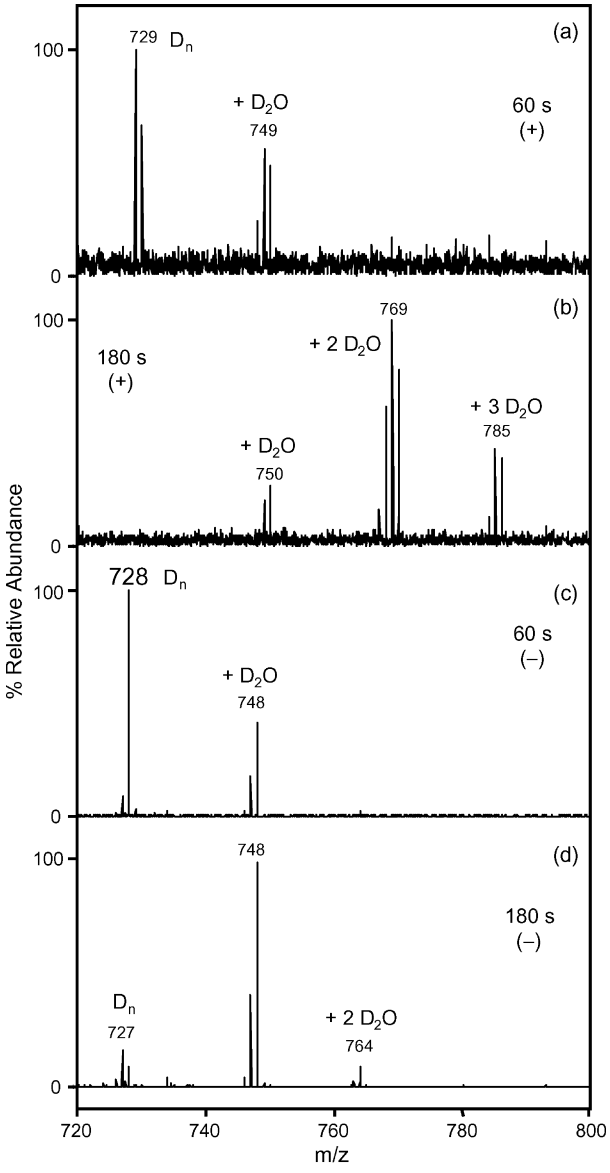

Fig. 7. FT-ICR mass spectrum showing ion-molecule reactions between D_2O and monoisotopically selected uranyl-monocitrate 2:1 complexes. Reaction times applied for the cation, $[(UO_2)_2(C_6H_5O_7)]^+$ (*m/z* 729) (a) 60s, (b) 180s, and (c) 60 s, and (d) 180s for the corresponding anion, $[(UO_2)_2(C_6H_4O_7)]^-$ (*m/z* 728).

time, fragmentation also occurs, leading primarily to the singly charged UO_2^+ cation (*m/z* 270). In contrast to the cation, the anion accumulates only one D_2O molecules, even after 180 s and less H/D exchange occurs. (Note that the experimental conditions were kept the same, except for the selection of cationic and anionic species.) The less prominent H/D exchange can easily be rationalized by the removal of the side chain carboxylic protons. The formation of a negative charge on the side chain may reduce the ability of the uranyl-citrate dimer complex to accept D_2O. Overall, these results provide strong additional support for the proposed structure of the uranyl-citrate dimer complex.

A similar trend but with a consistent shift in the number of associated D_2O molecules was observed for the anionic monocitrate complex, $[(UO_2)_2(C_6H_4O_7)]^-$ (Fig. 7). The cation $[(UO_2)_2(Cit)]^+$ (*m/z* 729) accumulates three D_2O molecules after a reaction time of 180 s (Fig. 7b), while the anion $[(UO_2)_2(C_6H_4O_7)]^-$ (*m/z* 728) accumulates only two (Fig. 7d). The number of H/D exchanges is consistently higher for the cation than for the anion. With the removal of one citrate ligand, one can speculate that one D_2O can be attached between the citrate side chain carbonyl (CH_2COOH) and the carboxylate oxygen. The other two D_2O molecules must than be attached to the uranyl cores. As expected, these core attachments can occur, albeit with less dominance, in the anion. On the other hand, the attachment to the side chain carboxyl is practically prohibited in the anion, while it is preferred in the cation.

4. Conclusions

The results presented in this work provide a good example of the use of ESI-MS to examine U(VI)-containing species, U(VI)-ligand stoichiometry and structure, and gas-phase chemistry. At a higher background and solvent pressure in a conventional 3D ion trap, uranyl-citrate complexes undergo a number of reactions that can complicate spectral interpretation, including H^+/X^+ exchange reactions where $X^+ = Na^+$ or K^+, the formation of adducts with common solution anions such as nitrate and chloride, as well as with excess ligand in solution. Overall, we can conclude that $H_3(UO_2)_3Cit_3$ is coordinately saturated, while $(UO_2)_3Cit_2$, $H_2(UO_2)_2Cit_2$, and $H(UO_2)_2(Cit)$ are not. The latter two species form cluster ions in the 3D ion trap with HNO_3, HCl, and neutral solvent molecules such as H_2O and CH_3CN. Isolation and application of collision energy to $H_3(UO_2)_3Cit_3$-containing ions results in fragmentation. However, $H_2(UO_2)_2Cit_2$ undergoes exchange or rearrangement reactions under similar conditions.

The mass spectra obtained at lower pressure in an FT-ICR cell are generally simpler and easier to interpret than the 3D ion trap spectra, with the added advantage that accurate mass measurements contribute significantly to the easier interpretation. Nevertheless, adduct formation with solvent molecules and alkali cations are also observed in the ICR trap together with association reactions between some SORI-CID fragments and of selected uranyl-citrate cations and anions with D_2O applied at higher pressure. Ion-molecule reactions with D_2O in the ICR cell proved to be especially useful in revealing structural differences among positively and negatively charged uranyl-citrate complexes. Overall, H/D exchange and D_2O addition is more pronounced for cations than for anions, and also for the less coordinated uranyl-monocitrate complex, $H(UO_2)_2(Cit)$, than for the more coordinated uranyl-citrate dimer complex, $H_2(UO_2)_2(Cit)_2$. The results also indicate that the uranyl-citrate complexes retain their main solvent-phase structural features in the gas-phase.

The results presented here provide excellent examples of the complicated ion formation and ion-molecule chemistry in trapping mass analyzers for inorganic ions. The growth of their clusters can be considered, especially in the 3D ion trap, as the formation of "dirty snowballs". This can complicate the assignments and structural studies of these species. The lower pressure of FT-ICR simplifies the spectra, so it is desirable to use different mass analyzers and different experimental conditions for these highly reactive ions. The results presented here also support the importance of ion-molecule reactions to reveal structural and electronic differences in complex ions.

Acknowledgements

The authors gratefully acknowledge support of this research by the National Institutes of Health through the University of Arizona-Northern Arizona University Native American Cancer Research Partnership funded through the Minority Institute Cancer Control Program of the National Cancer Institute (U54CA96281).

References

[1] J.K. Gibson, Int. J. Mass Spectrom. 214 (1) (2002) 1.
[2] C. Heinemann, H.H. Cornehl, H. Schwarz, J. Organometal. Chem. 501 (1–2) (1995) 201.
[3] J.K. Gibson, Organometallics 16 (1997) 4214.
[4] J.K. Gibson, J. Am. Chem. Soc. 120 (1998) 2633.
[5] J.K. Gibson, J. Mass. Spectrom. 34 (11) (1999) 1166.
[6] J. Marcalo, J.P. Leal, A. Pires de Matos, Organometallics 16 (1997) 4581.
[7] P.B. Armentrout, J.L. Beauchamp, Chem. Phys. 50 (1980) 27.
[8] H.H. Cornehl, C. Heinemann, J. Marcalo, A. Pires de Matos, H. Schwarz, Angew Chem. Int. Ed. Engl. 35 (8) (1996) 891.
[9] G.P. Jackson, F.L. King, D.E. Goeringer, D.C. Duckworth, J. Phys. Chem. A 106 (34) (2002) 7788.
[10] C. Moulin, N. Charron, G. Plancque, H. Virelizier, Appl. Spectrosc. 54 (6) (2000) 843.
[11] C. Moulin, B. Amekraz, D. Doizi, G. Plancque, V. Steiner, J. Inorg. Biochem. 86 (1) (2001) 347.
[12] C. Lamouroux, C. Moulin, J.C. Tabet, C.K. Jankowski, Rapid Commun. Mass Spectrom. 14 (2000) 1869.
[13] G.L. Gresham, A.K. Gianotto, P. de Harrington, L. Cao, J.R. Scott, J.E. Olson, A.D. Appelhans, M.J. Van Stipdonk, G.S. Groenewold, J. Phys. Chem. A 107 (41) (2003) 8530.
[14] M. Van Stipdonk, V. Anbalagan, W. Chien, G. Gresham, G. Groenewold, D. Hanna, J. Am. Soc. Mass Spectrom. 14 (2003) 1205.
[15] W. Chien, V. Anbalagan, M. Zandler, M.J. Van Stipdonk, J. Am. Soc. Mass Spectrom. 15 (2004) 777.
[16] M.J. Van Stipdonk, W. Chien, V. Anbalagan, G. Gresham, G. Groenewold, Int. J. Mass Spectrom. 237 (2004) 175.
[17] M.J. Van Stipdonk, W. Chien, V. Anbalagan, K. Bulleigh, D. Hanna, G. Groenewold, J. Phys. Chem. A 108 (47) (2004) 10448.

[18] M.J. Van Stipdonk, W. Chien, K. Bulleigh, Q. Wu, G.S. Groenewold, J. Phys. Chem. A 110 (2006) 959.
[19] G.S. Groenewold, K.C. Cossel, G.L. Gresham, A.K. Gianotto, A.D. Appelhans, J.E. Olson, M.J. Van Stipdonk, W. Chien, J. Am. Chem. Soc. 128 (9) (2006) 3075.
[20] G.R. Agnes, G. Horlick, Appl. Spectrosc. 46 (3) (1992) 401.
[21] S.P. Pasilis, PhD Dissertation, University of Arizona, Tucson, AZ, 2004.
[22] G.S. Groenewold, A.K. Gianotto, K.C. Cossel, M.J. Van Stipdonk, D.T. Moore, N. Polfer, J. Oomens, W.A. de Jong, L. Visscher, J. Am. Chem. Soc. 128 (2006) 4802.
[23] S.P. Pasilis, J.E. Pemberton, Inorg. Chem. 42 (21) (2003) 6793.
[24] S.P. Pasilis, A. Somogyi, K. Herrmann, J.E. Pemberton, J. Am. Soc. Mass Spectrom. 17 (2006) 230.
[25] C.Q. Jiao, D.R.A. Ranatunga, W.E. Vaugn, B.S. Freiser, J. Am. Soc. Mass Spectrom. 7 (1) (1996) 118.
[26] J.M. Wells, W.R. Plass, G.E. Patterson, Z. Ouyang, E.R. Badman, R.G. Cooks, Anal. Chem. 71 (1999) 3405.
[27] J.E. McClellan, J.P. Murphy, J.J. Mulholland, R.A. Yost, Anal. Chem. 74 (2002) 402.
[28] R.W. Vachet, J.A.R. Hartman, J.W. Gertner, J.H. Callahan, Int. J. Mass Spectrom. 204 (2001) 101.
[29] B.A. Perera, M.P. Ince, E.R. Talaty, M.J. Van Stipdonk, Rapid Commun. Mass Spectrom. 15 (2001) 615.
[30] B.A. Perera, A.L. Gallardo, J.M. Barr, S.M. Tekarli, V. Anbalagan, E.R. Talaty, M.J. Van Stipdonk, J. Mass Spectrom. 37 (2002) 401.
[31] G.E. Reid, R.A.J. O'Hair, M.L. Styles, W.D. McFayden, R.J. Simpson, Rapid Commun. Mass Spectrom. 12 (1998) 1701.
[32] T. Vaisar, C.L. Gatlin, F. Turecek, J. Am. Chem. Soc 118 (1996) 5314.
[33] T. Vaisar, C.L. Gatlin, F. Turecek, Int. J. Mass. Spectrom. Ion. Proc. 162 (1997) 77.
[34] S. Zhou, K.D. Cook, J. Am. Soc. Mass Spectrom. 11 (2000) 961.
[35] K.S. Rajan, A.E. Martell, Inorg. Chem. 4 (4) (1965) 462.
[36] M.T. Nunes, V.M.S. Gil, Inorg. Chim. Acta 129 (1987) 283.
[37] P.G. Allen, D.K. Shuh, J.J. Bucher, N.M. Edelstein, T. Reich, M.A. Denecke, H. Nitsche, Inorg. Chem. 35 (1996) 784.
[38] R.W. Vachet, J.A.R. Hartman, J.H. Callahan, J. Mass Spectrom. 33 (1998) 1209.
[39] R.W. Vachet, J.H. Callahan, J. Mass Spectrom. 35 (2000) 311.
[40] M.Y. Combariza, J. Am. Soc. Mass Spectrom. 13 (2002) 813.
[41] M.Y. Combariza, R.W. Vachet, Anal. Chim. Acta 496 (2003) 233.
[42] M.Y. Combariza, J.T. Fermann, R.W. Vachet, Inorg. Chem. 43 (2004) 2745.